Thermal expansion of select $M_{n+1}AX_n$ (M=early transition metal, A=A group element, X=C or N) phases measured by high temperature x-ray diffraction and dilatometry

T. H. Scabarozi,[1,2] S. Amini,[2] O. Leaffer,[2] A. Ganguly,[2] S. Gupta,[2] W. Tambussi,[1] S. Clipper,[1] J. E. Spanier,[2] M. W. Barsoum,[2] J. D. Hettinger,[1] and S. E. Lofland[1,a)]
[1]*Department of Physics and Astronomy, Rowan University, Glassboro, New Jersey 08028, USA*
[2]*Department of Materials Science and Engineering, Drexel University, Philadelphia, Pennsylvania 19104, USA*

(Received 18 July 2008; accepted 4 October 2008; published online 14 January 2009)

Herein we report on a systematic investigation of the thermal expansion of select $M_{n+1}AX_n$ phases. The bulk dilatometric thermal expansion coefficient α_{dil} was measured in the 25–1200 °C temperature range and the thermal expansion of more than 15 of these phases was studied by x-ray diffraction in the 25–800 °C temperature range. The coefficient of thermal expansion for the a axis α_a ranged between $(2.9\pm0.1)\times10^{-6}$ °C^{-1} (Nb_2AsC) and $(12.9\pm0.1)\times10^{-6}$ °C^{-1} (Cr_2GeC) while the coefficient for the c axis (α_c) ranged between $(6.4\pm0.2)\times10^{-6}$ °C^{-1} (Ta_2AlC) and $(17.6\pm0.2)\times10^{-6}$ °C^{-1} (Cr_2GeC). Weak anisotropy in the thermal expansion was seen in most phases, with the largest value of α_c/α_a belonging to Nb_2AsC. The Grüneisen parameters along the a and c directions were calculated from *ab initio* values for the elastic compliances and were relatively isotropic. A good correlation was found between the thermal expansion anisotropy and the elastic constant c_{13} and we conclude that the anisotropy in thermal expansion is related to the bonding between the $M-A$ elements. © *2009 American Institute of Physics*.
[DOI: 10.1063/1.3021465]

I. INTRODUCTION

The $M_{n+1}AX_n$ (MAX) phases ($n=1-3$) are layered hexagonal compounds, in which near close-packed layers of M (early transition metals) are interleaved with layers of group A element (mostly IIIA and IVA), with the X-atoms (C and/or N) filling the octahedral sites between the M layers. Most of these phases were synthesized in powder form in the 1960s by Nowotny.[1] At this time it is fairly well established that these phases have an unusual and sometimes unique combination of properties.[2–16] They are elastically stiff, have relatively low thermal expansion coefficients, and have good thermal and electrical conductivities.[2,17] They are relatively soft, with Vickers hardness values of 2–8 GPa, easily machinable, thermal shock, and damage tolerant. Some are fatigue, creep, and oxidation resistant.[18] At higher temperatures, they can undergo a brittle-to-plastic transition.[12] Some, such as Ti_2AlC, are exceptionally oxidation resistant and are candidate materials for high temperature structural industrial applications.[19]

Elastic measurements indicate that these materials are stiff, particularly in shear. In particular, some M_2AX (211) materials, such as Ti_2SC (Ref. 20), show enhanced elastic properties although they are not as readily machinable as other MAX-phase materials. It is believed that the origin of the increased modulus in this material is due to stronger $M-A$ bonds. A similar study done on Nb_2AsC showed higher compressibility in the a-direction than the c-direction, which can be associated with the position of Nb being closer to the As.[21]

In the M_3AX_2 (312) materials, increased stiffness is a result of a higher fraction of the stronger $M-X$ bonds. The most studied MAX phase, Ti_3SiC_2, exhibits weak elastic anisotropy associated with two different Ti–C bonds and Si vibrating preferentially along the a axis.[22,23] Compressibility studies[24] of $Ti_3Si_{1-x}Ge_xC_2$ found solid-solution softening occurred while investigations of Ti_3AlCN and $Ti_2AlC_{0.5}N_{0.5}$ suggest the formation of vacancies on both the Al and N sites leading to the decrease in bulk moduli.[25] In M_4AX_3 compounds, there are even less weaker $M-A$ bonds and the $M-X$ bonds are shorter and stiffer, as reported for Ti_4AlN_3.[26] An exception is seen in Ta_4AlC_3 where high-pressure diffraction studies reveal little anisotropy in compressibility attributed to lattice softening due to differences in atomic packing.[27] The purpose of this paper is to further investigate the role of bonding anisotropies in the MAX phases by measuring the thermal expansion of a large number of these phases by high temperature x-ray diffraction (XRD).

II. EXPERIMENTAL DETAILS

All samples were synthesized by either hot isostatic pressing or hot pressing, providing fully dense and predominantly single phase microstructures. Details of processing of Cr_2AlC and Ta_2AlC can be found in Ref. 18, $Ti_2Al(C_{0.5}N_{0.5})$ in Ref. 28, $Ti_3Al(C_{0.5}N_{0.5})_2$ in Ref. 29, Ti_3SiC_2 in Ref. 4, Ti_3GeC_2 and $Ti_3Si_{0.25}Ge_{0.75}C_2$ in Ref. 30, V_2AlC, V_2AsC, Nb_2AlC, Nb_2SnC, Ti_2AlC, and Hf_2InC in Ref. 31, Ti_3AlC_2 and Ti_4AlN_3 in Ref. 32, Nb_2AsC in Ref. 33, Cr_2GeC in Ref. 34, Ti_2AlN in Ref. 35, and Ti_2SC in Ref. 36.

To synthesize the V_2GeC samples, V and C powders (Alfa Aesar, Ward Hill, MA) and Ge powder (Cerac Inc.,

a)Electronic mail: lofland@rowan.edu.

Milwaukee, WI) were mixed in stoichiometric proportions, ball milled for 12 h, and dried at 150 °C for 24 h. The powder mixtures were sealed in graphite foil, placed in a graphite die, heated at 10 °C/min in a graphite-heated vacuum atmosphere hot press (Series 3600, Centorr Vacuum Industries, Somerville, MA), annealed at 875 °C for 3 h, and then hot pressed at 1350 °C for 6 h under a load that corresponded to a stress of 45 MPa.

The bulk thermal expansion measurements were performed with a dilatometer (model 1161, Anter Corporation Unitherm, Pittsburgh, PA) on electric-discharge machined bar-shaped specimens with dimensions of $\sim 3 \times \sim 3 \times \sim 20$ mm^3. The heating and cooling rates were set at 3 K/min. To avoid oxidation, the dilatometric experiments were carried out under an atmosphere of ultrahigh pure Ar gas.

The high-temperature XRD diffractometer (Scintag X_2) was configured with a furnace (Edmund Bühler HDK-2.3). The diffractometer utilized Cu Kα radiation (40 mA and 45 kV) and a Si(Li) Peltier-cooled solid-state detector. Data were taken from 5° – 100° in steps of 0.02° with hold times of 1 or 2 s/step. MAX phase powders were mixed together with Si and Cu powders at ratios such that the intensity values of the strongest diffraction lines of the various materials were roughly equal at room temperature. The Si powder was mixed with the MAX phase to serve as a standard for alignment. The Cu powder was used to measure the mixture temperature via knowledge of its thermal expansion. From a slurry mixture, a 50–75 μm coating was applied either on a substrate (Zr, Mo, or sapphire) or directly on the Pt/Rh-10% heating element. A Pt/Rh-30% thermocouple was bonded to the back of the heater for temperature control. To minimize possible oxidation, the measurements were carried out either under vacuum (10^{-4} Torr) or in a He atmosphere from room temperature to 1000 °C. The heating rate was 20 °C/min with a 15 min hold time prior to each scan. Spectra were fit to a Pearson7 line shape by Scintag software DMSNT 1.36b. Lattice refinements were done with XLAT.[37] The thermal expansion for Si was taken from Ref. 38 and that of Cu from NIST.[39]

Ab initio density functional calculations were conducted with the Vienna *ab initio* simulation package (VASP) (Ref. 40) and the MEDEA (Ref. 41) interface. All calculations were carried out using the projector augmented wave[42,43] and the generalized gradient approximation.[44] Relaxed structures were calculated and energies were converged with respect to the *k*-mesh with MEDEA's convergence method. Subsequent calculations were carried out with the *k*-mesh resulting from the convergence. Elastic properties were calculated with MEDEA's mechanical and thermomechanical module,[45] which calculates the stress tensor from changes in energy when the unit cell is strained. Strains of 0.005, 0.01, and 0.02 were simulated. The reported elastic constants are from a least-squares fitting of the values calculated for each strain.

III. RESULTS AND DISCUSSION

Figure 1 shows the dilatometric thermal expansion α_{dila} as a function of temperature T for select compositions. The curves are shifted vertically for clarity. The α_{dila} values, reported in column 9 of Table I, were calculated by a least-squares fit of both the heating and cooling curves in the temperature range mentioned therein. Also included in the table are previously reported values.

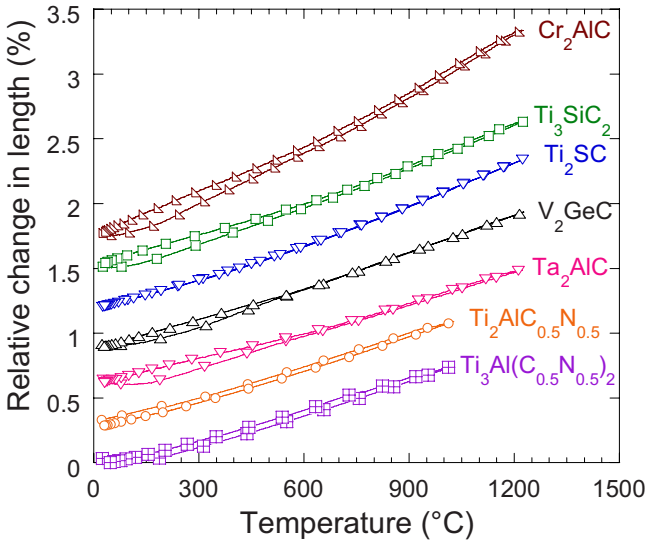

FIG. 1. (Color online) Thermal expansion as a function of temperature for selected MAX phases from dilatometer measurements. Curves have been shifted vertically for clarity.

Figure 2 shows several XRD patterns of Cr_2GeC at different temperatures. It is clearly seen the Cr_2GeC and Cu peaks noticeably shift to the left with increasing temperature. The shift for Si is much less indicating that, (i) its thermal expansion is smaller and, (ii) more importantly, that the sample height remains effectively constant, minimizing corrections due to focus.

Figure 3 shows the temperature dependencies and estimated errors of the lattice constants of more than 15 MAX

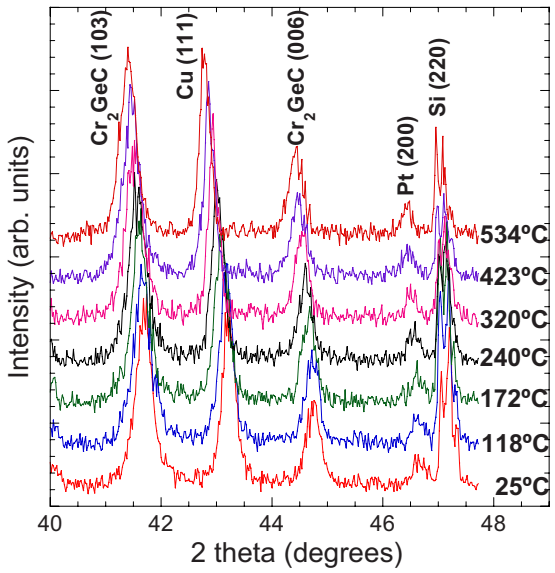

FIG. 2. (Color online) High temperature XRD of Cr_2GeC. Shifting peaks can be seen due to atomic spacing increasing as a function of temperature. Silicon and copper are used as internal standards for alignment and temperature determination, respectively. The Pt peak is associated with the heater strip.

TABLE I. Lattice parameters and thermal expansions for the MAX-phases studied by XRD (numbers in parentheses are estimated standard deviations in the last significant figure of the refined parameter).

									Other work			
Compound	a (Å)	c (Å)	α_a (10^{-6} °C^{-1})	α_c (10^{-6} °C^{-1})	Anisotropy (α_c/α_a)	c/a	α_{av} (10^{-6} °C^{-1})	α_{dila} (10^{-6} °C^{-1})	α_a (10^{-6} °C^{-1})	α_c (10^{-6} °C^{-1})	α_{av} (10^{-6} °C^{-1})	Ref.
Ti_4AlN_3	2.9884(1)	23.3810(35)	8.3(2)	8.3(9)	1.00(1)	7.824	8.3(5)	9.7(2)[a]	9.6(1)[b]	8.8(1)[b]	9.4(1)[b]	46
								9.1(5)				
								9.1(2)[c]	8.4(1)[d]	9.3(10)[d]	8.6(4)[d]	22
Ti_3SiC_2	3.0663(1)	17.6510(18)	8.9(1)	10.0(2)	1.12(2)	5.756	9.3(2)	9.1(2)[e]	8.6(1)[b]	9.7(1)[b]	9.1(2)[b]	23
Ti_3AlCN	3.0442(2)	18.3890(11)	6.0(2)	11.3(2)	1.89(2)	6.041	7.8(2)	7.5(5)				
Ti_3GeC_2	3.0873(2)	17.8071(10)	8.1(2)	9.7(2)	1.20(3)	5.768	8.6(2)	7.8(2)				
$Ti_3Si_{0.25}Ge_{0.75}C_2$	3.0855(5)	17.7960(18)	8.8(6)	11.1(3)	1.27(6)	5.768	9.6(5)					
Ti_3AlC_2	3.0698(1)	18.4998(2)	8.3(1)	11.1(1)	1.33(1)	6.026	9.2(1)	9.0(2)[f]				
								7.9(5)				
Ti_2AlCN	3.0247(1)	13.6046(5)	8.4(1)	8.8(1)	1.05(2)	4.498	8.5(1)	10.5(2)[a]				
								8.2(2)[g]				
Ti_2AlN	2.9872(2)	13.6108(6)	10.6(2)	9.75(2)	0.92(3)	4.556	10.3(2)	8.8(2)[a]	8.6(2)[d]	7.0(5)[d]	8.1(5)[d]	28
Ti_2SC	3.2046(1)	11.2092(3)	8.6(1)	8.7(2)	1.01(2)	3.498	8.7(1)	9.3(6)	8.5(5)[d]	8.8(2)[d]	8.6(6)[d]	47
V_2AlC	2.9176(3)	13.1281(9)	9.1(2)	10.0(7)	1.10(16)	4.500	9.4(10)	9.4(5)	9.34(5)[d]	9.48(4)[d]	9.39(5)[d]	48
V_2GeC	3.0034(1)	12.2527(9)	6.9(1)	15.8(3)	2.27(1)	4.080	9.9 (2)	9.4(6)				
V_2AsC	3.1127(1)	11.3884(4)	7.2(1)	14.0(1)	1.92(1)	3.659	9.5(1)					
Cr_2GeC	2.9500(2)	12.1010(10)	12.9(1)	17.6(2)	1.37(1)	4.102	14.5(2)	9.5(5)				
Cr_2AlC	2.8571(2)	12.8208(6)	12.8(3)	12.1(1)	0.94(3)	4.487	12.6(2)	12.8(5)				
Nb_2SnC	3.2376(2)	13.8135(4)	6.6(4)	14.5(2)	2.17(2)	4.267	9.3(3)	7.8(2)[h]				
								7.5(2)[g]				
Nb_2AlC	3.1063(1)	13.8783(11)	8.8(2)	6.8(3)	0.78(6)	4.468	8.1(2)	8.7(2)[i]				
Nb_2AsC	3.3235(1)	11.9036(3)	2.9(1)	10.6(1)	2.57(1)	3.582	5.5(1)	7.3(5)				
Hf_2InC	3.3085(1)	14.7351(10)	7.2(1)	7.6(2)	1.05(3)	4.454	7.3(2)	7.6(2)[j]				
Ta_2AlC	3.0804(2)	13.8630(7)	9.2(2)	6.4(2)	1.43(3)	4.5	8.3(2)	7.2(6)				
								8.8(2)[g]				
Ti_2AlC								8.2(2)[a]	7.1(3)[d]	10.0(5)[d]	8.1(5)[d]	28

[a]Reference 28.
[b]Neutron diffraction.
[c]Reference 22.
[d]XRD.
[e]Reference 23.
[f]Reference 49.
[g]Reference 2.
[h]Reference 50.
[i]Reference 51.
[j]Reference 52.

phases measured in this work. Table I lists the values of α_a and α_c, as well as previously reported high-temperature XRD or neutron diffraction results. The values obtained from diffraction (column 8) are compared with the dilatometric values (column 9) by assuming the average coefficient of thermal expansion, $\alpha_{av}=(2/3\ \alpha_a+1/3\ \alpha_c)$. In most cases, the results agree reasonably well with those of other measurements. For example, the presently reported values for α_a and α_c for Ti_3SiC_2, $(8.9\pm0.1)\times10^{-6}$ and $(10.0\pm0.2)\times10^{-6}$ °C^{-1}, respectively, are in excellent agreement with previous results.[22,23] The same is true for V_2AlC and Ti_2SC.[53,54] The agreement is not as good for Ti_2AlN,[28] which may reflect variations in stoichiometry.[35,55]

Figure 4(a) compares α_{av} of the MAX phases (solid circles) with those of their corresponding MX (open squares). From this plot it is reasonable to conclude that a relationship exists between the two. With the notable exception of Nb_2AsC, which is unusual, as noted above, the α values of the binaries are indeed lower than those of the corresponding MAX phase, suggesting that, on the average, the $M-X$ bonds are stronger than the $M-A$ bonds, a not too surprising conclusion.

The anisotropy ratio (α_c/α_a), listed in column 6 of Table I, for the most part, is >1, as might be anticipated since the c direction involves the relatively weaker $M-A$ bonds. However, as seen in Fig. 5(a), the anisotropy is mostly a function of the A-group element.

In an isotropic system, the volume thermal expansion α_V is given by

$$\alpha_V = \gamma\frac{c_v}{BV} \tag{1}$$

where γ is the Grüneisen parameter, a measure of the anharmonicity, which gives rise to thermal expansion, B is the bulk modulus, V is the molar volume, and c_V is the molar specific heat at constant volume. In Table II are the lattice constants a, B, and γ for the cubic binary carbides, assuming that the Dulong–Petit law applies, i.e., $c_V=3mR$, where m is

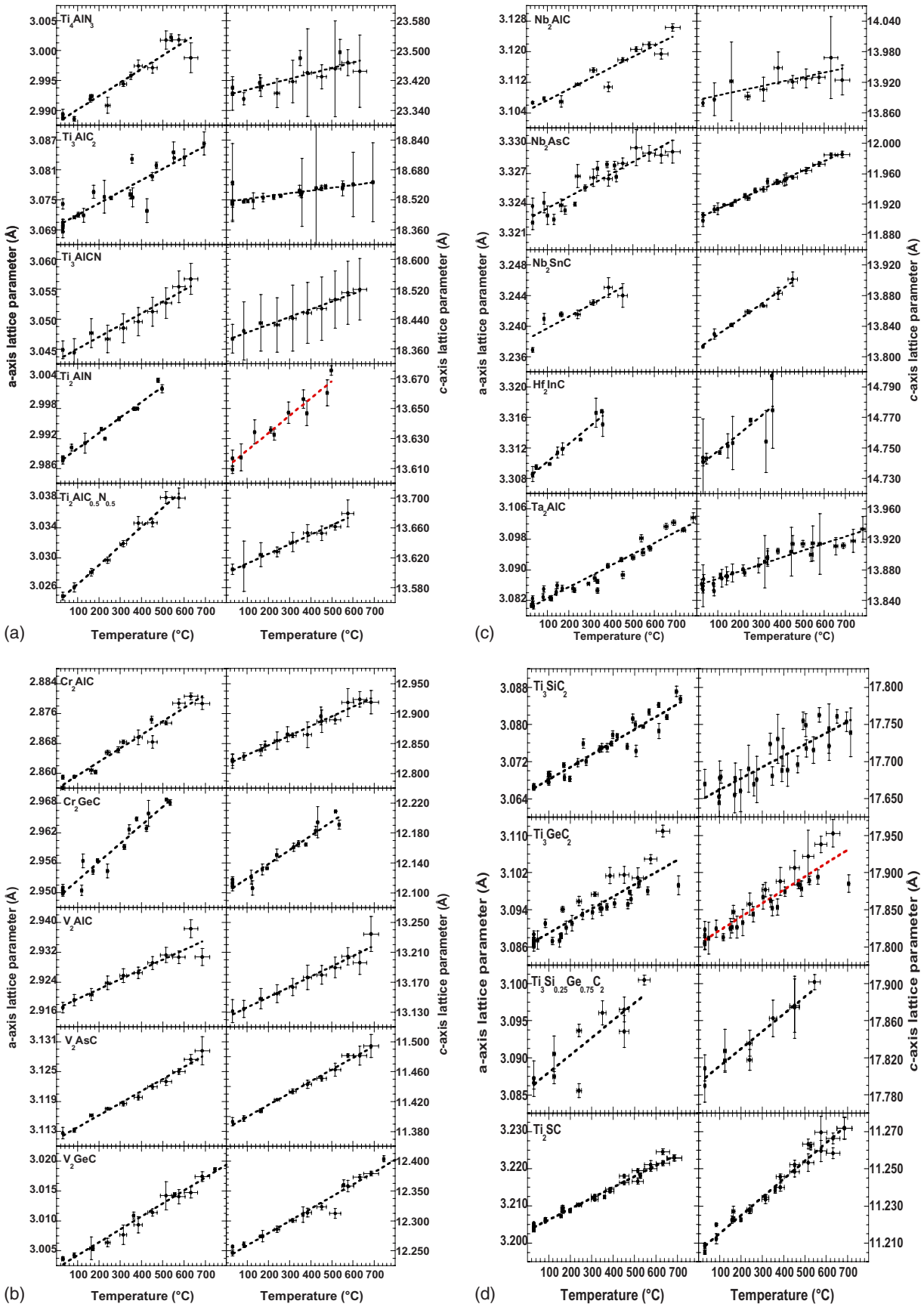

FIG. 3. (Color online) Temperature dependence of the lattice constants for (a) various Ti–Al–*X* phases, (b) various M_2AC (M=Cr or V, A=Al, As, or Ge) phases, (c) various M_2AC (M=Nb, Hf, or Ta, A=Al, As, In, or Sn) phases, and (d) various Ti–A–C (A=Si, Ge, or S) phases.

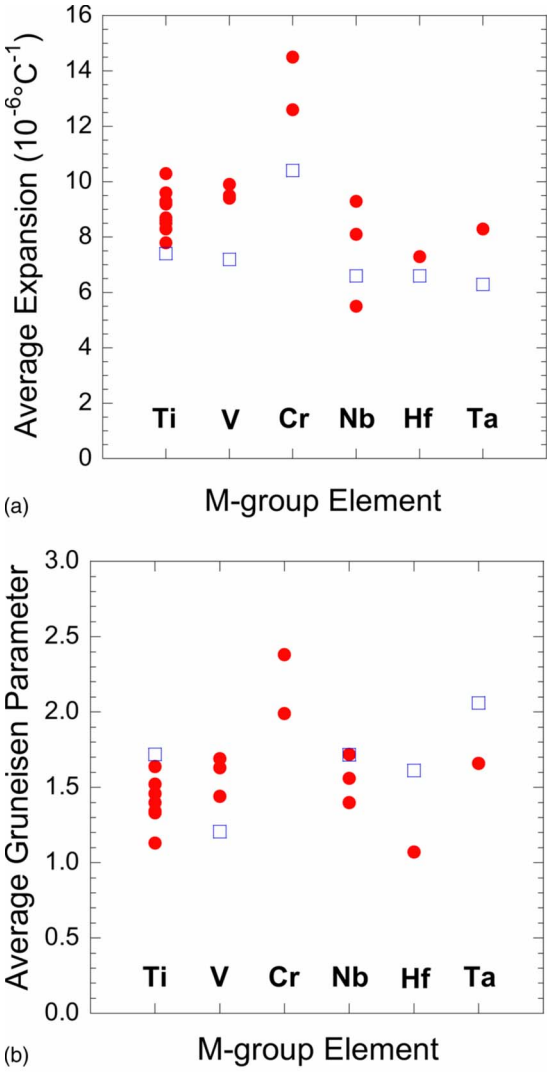

FIG. 4. (Color online) (a) Average thermal expansion as a function of the *M*-group element for MAX phase materials (solid markers). (b) Average Grüneisen parameter as a function of *M*-group element for MAX phase materials (solid markers). In both figures, open markers represent the values for the respective binary carbide.

the number of atoms per unit cell and R is the ideal gas constant. Where possible, we used XRD data for the thermal expansion and diamond anvil cell measurements of the bulk moduli. For the most part, the values are between 1.5 and 2, as expected for metallic compounds. The outlier is VC, which is always substoichiometric.[63]

When the average Grüneisen parameters of the ternaries and binaries are plotted on the same figure [Fig. 4(b)], there is little correlation between the two, which indirectly implicates the *A*-group element in the thermal expansion anisotropies observed. This notion can be tested further. In a system with axial symmetry (i.e., hexagonal, tetragonal, or rhombohedral), one can write down the Grüneisen parameters for the a and c directions, as γ_a and γ_c, respectively, as

$$\gamma_a = \frac{V}{C_v}[(c_{11}+c_{12})\alpha_a + c_{13}\alpha_c], \tag{2a}$$

TABLE II. Lattice parameter and properties for binary carbides.

Binary carbide	a (Å)	α (10^{-6} °C^{-1})	B (GPa)	γ
TiC	4.328	9.44[a]	248[b]	1.72
VC	4.153	7.3[c]	258[d]	1.20
ZrC	4.698	7.37[a]	195[e]	1.35
NbC	4.47	7.74[f]	274[g]	1.71
HfC	4.639	7.37[f]	242[h]	1.61
TaC	4.456	7.45[f]	345[e]	2.06
Cr_3C_2		10.4[c]		

[a]Reference 56.
[b]Reference 57.
[c]Reference 58.
[d]Reference 59.
[e]Reference 27.
[f]Reference 60.
[g]Reference 61.
[h]Reference 62.

$$\gamma_c = \frac{V}{C_v}(2c_{13}\alpha_a + c_{33}\alpha_c), \tag{2b}$$

where c_{ij} are the elastic stiffness constants.[64]

Since MAX phase single crystals large enough for the measurement of the various elastic constants do not exist to date, one must rely on *ab initio* calculations for those constants to proceed with the analysis. Nonetheless, one can check the validity of the calculated numbers by comparing them with the measured values for B, the shear modulus G, and the compressibilities along the a and c directions, κ_a and κ_c, respectively. The Voigt averages, which provide a method of connecting the calculated elastic constants to the measured parameters, yield

$$B = \frac{2(c_{11}+c_{12})+4c_{13}+c_{33}}{9}, \tag{3a}$$

$$G = \tfrac{1}{30}(7c_{11}-5c_{12}+2c_{33}-4c_{13}+12c_{44}). \tag{3b}$$

For hydrostatic compression, one finds

$$\kappa_a = \frac{c_{33}-c_{13}}{c_{33}(c_{11}+c_{12})-2c_{13}^2}, \tag{4a}$$

$$\kappa_c = \frac{c_{11}+c_{12}-2c_{13}}{c_{33}(c_{11}+c_{12})-2c_{13}^2}. \tag{4b}$$

The calculated elastic constants, as well as the measured values, are listed in Table III.

While the agreement between the calculated and measured values for B, G, κ_a, and κ_c is not exact,[16,17,24–26,49,66–68] they are generally close except for the latter two, which are particularly sensitive to the value of c_{13}. It is to be noted that there has been, in general, excellent agreement between the calculated and observed Raman spectra,[69] further evidence that the calculated elastic constants are quite reasonable.

As seen in Table IV, the calculated γ values from $c_V = 3mR$, where $m=4(n+1)$ for the MAX phases, range between 1.5 and 2.5, as expected for metallic compounds. Figure 4(b) shows that the average Grüneisen parameter is ef-

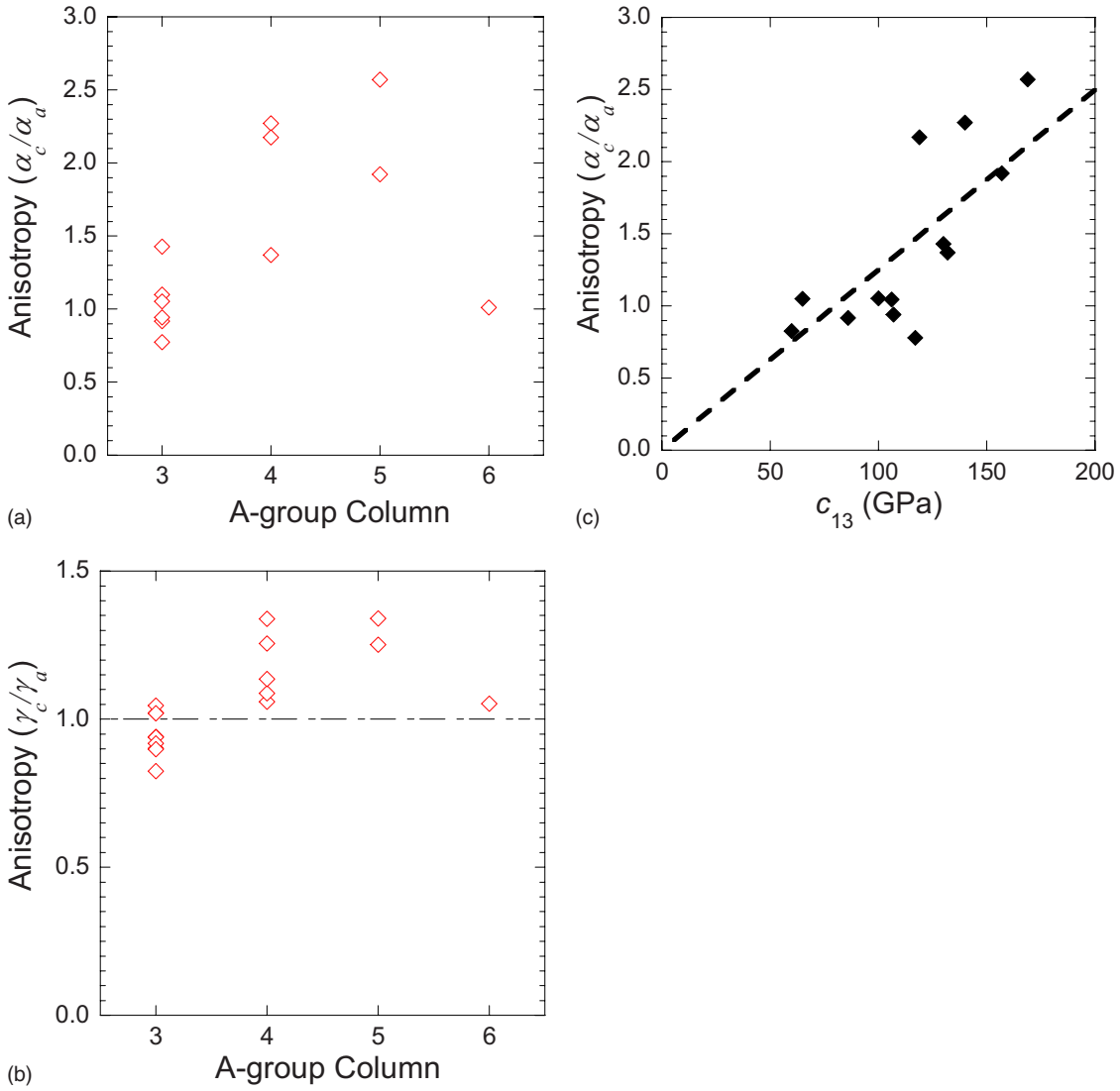

FIG. 5. (Color online) (a) Anisotropy in thermal expansion vs *A*-group elements. (b) Anisotropy in the Grüneisen parameter vs *A*-group column. (c) The compliance tensor element c_{13} vs the *A*-group column.

fectively constant for a given *M*-group element but does not obviously relate to that of the corresponding binary carbide.

Comparing Figs. 4(a) and 4(b), one notices a direct correlation between α and γ. From Eq. (1), $\alpha \propto \gamma/BV$ and, thus, BV is effectively constant for all MAX phases of any given family. This relationship has been found in a variety of other class of solids such as halides,[70] oxides,[70] and chalcogenides,[71] as well as for binary carbides.[53] The correlation for the latter, however, has not been nearly as good as the results shown here for the ternaries. The discrepancies for the binary carbides have been partly attributed to stoichiometry and microstructure.[72]

Note that the anisotropies in the calculated γ values [Fig. 5(b)] are small compared to those of the corresponding α values [Fig. 5(a)]. This reflects the fact that the anharmonicity is relatively isotropic and suggests that the anisotropy in thermal expansion is related predominantly to the anisotropy in the elastic constants, which must be a consequence of the bonding of the *M* element to the A group. Confirming this notion is the fact that the anisotropy in α of the 211 phases correlates well with c_{13} [Fig. 5(c)]. This is not too surprising since c_{13} compares the bonding strengths in the *a* and *c* planes of hexagonal crystals. In Fig. 5(c) Nb_2AlC is an outlier, most probably a direct result of the exceptionally strong Nb–Al bonds.[73] Nb_2SnC is also an outlier, but in the opposite sense, in that α_c is considerably larger than α_a. Using the same logic, it is reasonable to conclude that the Nb–Sn bonds are weaker than average, which is not reflected in c_{13}. Lastly we note that the good correlation found in Fig. 5(c) indirectly confirms the validity of both the thermal expansion measurements and *ab initio* calculations, which are in good agreement with other similar calculations on the MAX phases given in the literature.[74–81]

IV. CONCLUSIONS

We measured the thermal expansion of a number of MAX phases. Overall, anisotropy between the *a* and *c* axes was mild for most of them, the largest belonging to Nb_2AsC. The Grüneisen parameters determined from *ab initio* calculated elastic constants are consistent with expectations for metals and are relatively isotropic. The anisotropy in thermal

TABLE III. Elastic properties of the measured MAX-phases in this study.

	Calculated elastic parameters										Measured elastic parameters				
Compound	c_{11} (GPa)	c_{12} (GPa)	c_{13} (GPa)	c_{33} (GPa)	c_{44} (GPa)	B (GPa)	G (GPa)	$10^3\kappa_a$ (GPa^{-1})	$10^3\kappa_c$ (GPa^{-1})	Ref.	B^* (GPa)	$10^3\kappa_a$ [a] (GPa^{-1})	$10^3\kappa_c$ [a] (GPa^{-1})	Ref.	G [b] (GPa)
Ti_4AlN_3	405	94	102	361	160	196	153	1.63	1.85	[c]	216(2)	1.30	1.60	26	127[d]
Ti_3SiC_2	365	125	120	375	122	204	122	1.65	1.61	[c]	206(6)	0.92	2.02	52	138[e]
Ti_3GeC_2	355	143	80	404	172	191	144	1.72	1.79	[c]	197(4)	1.60	1.60	24	141[e]
Ti_3AlC_2	361	75	70	299	124	161	132	1.90	2.46	65	226(3)	0.80	2.10	25	124[f]
Ti_2AlN	312	69	86	283	127	154	120	2.12	2.25	[c]	169(3)	1.80	1.90	51	120[g]
Ti_2SC	339	90	100	354	162	179	139	1.93	1.74	[c]	191(3)	1.42	2.20	46	125[h]
V_2AlC	346	71	106	314	151	175	136	1.92	1.89	65	201(3)	1.00	2.20	16	116[i]
V_2GeC	311	122	140	291	158	191	116	1.74	1.76	[c]					
V_2AsC	334	109	157	321	170	204	128	1.77	1.39	[c]					
Cr_2GeC	315	145	132	339	91	199	91	1.71	1.62	[c]					80[j]
Cr_2AlC	384	79	107	382	147	193	146	1.79	1.62	65	165(2)	2.10	1.70	16	105[i]
Nb_2SnC	268	86	119	267	98	161	89	2.24	1.75	[c]					
Nb_2AlC	341	94	117	310	150	183	129	1.80	1.87	65	209(2)	1.40	1.40	16	117[i]
Nb_2AsC	334	104	169	331	167	209	127	1.84	1.14	[c]	224(2)	1.30	0.70	21	
Hf_2InC	284	69	65	243	91	134	99	2.30	2.88	[c]					
Ta_2AlC	339	113	130	326	154	194	126	1.73	1.69	[c]					
Ti_2AlC	308	55	60	270	111	137	117	2.31	2.68	65	186(2)	1.10	2.40	16	118[i]

[a]Determined from diamond-anvil cell XRD studies.
[b]Determined from velocity of sound measurements.
[c]Present work.
[d]Reference 66.
[e]Reference 30.
[f]Reference 49.
[g]Reference 27.
[h]Reference 36.
[i]Reference 17.
[j]Reference 34.

TABLE IV. Calculated Grüneisen parameters of MAX phase materials.

Compound	γ_a	γ_c	$\langle\gamma\rangle$	Anisotropy (γ_c/γ_a)
Ti_4AlN_3	1.36	1.28	1.33	0.94
Ti_3SiC_2	1.61	1.70	1.64	1.06
Ti_3GeC_2	1.42	1.54	1.46	1.09
Ti_3AlC_2	1.33	1.36	1.34	1.02
Ti_2AlN	1.55	1.46	1.52	0.94
Ti_2SC	1.38	1.45	1.40	1.05
V_2AlC	1.41	1.48	1.44	1.05
V_2GeC	1.51	1.89	1.63	1.25
V_2AsC	1.56	1.95	1.69	1.25
Cr_2GeC	2.27	2.58	2.38	1.14
Cr_2AlC	1.98	2.01	1.99	1.02
Nb_2SnC	1.54	2.06	1.72	1.34
Nb_2AlC	1.62	1.46	1.56	0.90
Nb_2AsC	1.26	1.69	1.40	1.34
Hf_2InC	1.10	1.01	1.07	0.92
Ta_2AlC	1.71	1.54	1.66	0.90
Ti_2AlC	2.41	1.99	2.27	0.83

expansion is related to the bonding between $M-A$, while the magnitude of the thermal expansion is controlled by $M-X$ bonding. The bulk modulus of any given family of compounds is inversely related to the unit cell volumes.

ACKNOWLEDGMENTS

We gratefully acknowledge the support of the National Science Foundation through Grant No. DMR-0503711. The authors acknowledge the support of C. Lunk for assistance with the XRD equipment.

[1]G. Nowotny, Prog. Solid State Chem. **2**, 27 (1970).
[2]M. W. Barsoum, Prog. Solid State Chem. **28**, 201 (2000).
[3]M. W. Barsoum, D. Brodkin, and T. El-Raghy, Scr. Mater. **36**, 535 (1997).
[4]M. W. Barsoum and T. El-Raghy, J. Am. Ceram. Soc. **79**, 1953 (1996).
[5]M. W. Barsoum and T. El-Raghy, J. Mater. Synth. Process. **5**, 197 (1997).
[6]M. W. Barsoum and T. El-Raghy, Metall. Mater. Trans. A **30**, 363 (1999).
[7]M. W. Barsoum, T. El-Raghy, C. J. Rawn, W. D. Porter, H. Wang, A. Payzant, and C. Hubbard, J. Phys. Chem. Solids **60**, 429 (1999).
[8]M. W. Barsoum, L. Farber, T. El-Raghy, and I. Levin, Metall. Mater. Trans. A **30**, 1727 (1999).
[9]M. W. Barsoum, G. Yaroschuck, and S. Tyagi, Scr. Mater. **37**, 1583 (1997).
[10]T. El-Raghy and M. W. Barsoum, J. Am. Ceram. Soc. **82**, 2849 (1999).
[11]M. W. Barsoum, T. El-Raghy, and L. Ogbuji, J. Electrochem. Soc. **144**, 2508 (1997).
[12]T. El-Raghy, M. W. Barsoum, A. Zavaliangos, and S. R. Kalidindi, J. Am. Ceram. Soc. **82**, 2855 (1999).
[13]T. El-Raghy, A. Zavaliangos, M. W. Barsoum, and S. R. Kalidindi, J. Am. Ceram. Soc. **80**, 513 (1997).
[14]L. Farber, M. W. Barsoum, A. Zavaliangos, T. El-Raghy, and I. Levin, J.

Am. Ceram. Soc. **81**, 1677 (1998).
[15]I. M. Low, S. K. Lee, B. Lawn, and M. W. Barsoum, J. Am. Ceram. Soc. **81**, 225 (1998).
[16]B. Manoun, R. P. Gulve, S. K. Saxena, S. Gupta, M. W. Barsoum, and C. S. Zha, Phys. Rev. B **73**, 024110 (2006).
[17]J. D. Hettinger, S. E. Lofland, P. Finkel, T. Meehan, J. Palma, K. Harrell, S. Gupta, A. Ganguly, T. El-Raghy, and M. W. Barsoum, Phys. Rev. B **72**, 115120 (2005).
[18]M. W. Barsoum and M. Radovic, *Encyclopedia of Materials: Science and Technology*, edited by K. H. J. Buschow (Elsevier, Amsterdam, 2004).
[19]M. W. Barsoum, N. Tzenov, A. Procopio, T. El-Raghy, and M. Ali, J. Electrochem. Soc. **148**, C551 (2001).
[20]T. H. Scabarozi, S. Amini, P. Finkel, O. D. Leaffer, J. E. Spanier, M. W. Barsoum, M. Drulis, H. Drulis, W. M. Tambussi, J. D. Hettinger, and S. E. Lofland, J. Appl. Phys. **104**, 033502 (2008).
[21]R. S. Kumar, S. Rekhi, A. L. Cornelius, and M. W. Barsoum, Appl. Phys. Lett. **86**, 111904 (2005).
[22]B. Manoun, S. K. Saxena, H. P. Liermann, and M. W. Barsoum, J. Am. Ceram. Soc. **88**, 3489 (2005).
[23]M. W. Barsoum, T. El-Raghy, C. J. Rawn, W. D. Porter, H. Wang, E. A. Payzant, and C. R. Hubbard, J. Phys. Chem. Solids **60**, 429 (1999).
[24]B. Manoun, H. Yang, S. K. Saxena, A. Ganguly, M. W. Barsoum, B. E. Bali, Z. X. Liu, and M. Lachkar, J. Alloys Compd. **433**, 265 (2007).
[25]B. Manoun, S. K. Saxena, G. Hug, A. Ganguly, E. N. Hoffman, and M. W. Barsoum, J. Appl. Phys. **101**, 113523 (2007).
[26]B. Manoun, S. K. Saxena, and M. W. Barsoum, Appl. Phys. Lett. **86**, 101906 (2005).
[27]B. Manoun, S. K. Saxena, T. El-Raghy, and M. W. Barsoum, Appl. Phys. Lett. **88**, 201902 (2006).
[28]T. El-Raghy, M. Ali, and M. W. Barsoum, Metall. Mater. Trans. A **31A**, 1857 (2000).
[29]M. Radovic, A. Ganguly, M. W. Barsoum, T. Zhen, P. Finkel, S. R. Kalidindi, and E. Lara-Curzio, Acta Mater. **54**, 2757 (2006).
[30]P. Finkel, B. Seaman, K. Harrell, J. Palma, J. D. Hettinger, S. E. Lofland, A. Ganguly, M. W. Barsoum, Z. Sun, S. Li, and R. Ahuja, Phys. Rev. B **70**, 085104 (2004).
[31]S. E. Lofland, J. D. Hettinger, K. Harrell, P. Finkel, S. Gupta, M. W. Barsoum, and G. Hug, Appl. Phys. Lett. **84**, 508 (2004).
[32]P. Finkel, M. W. Barsoum, J. D. Hettinger, S. E. Lofland, and H. I. Yoo, Phys. Rev. B **67**, 235108 (2003).
[33]S. E. Lofland, J. D. Hettinger, T. Meehan, A. Bryan, P. Finkel, S. Gupta, M. W. Barsoum, and G. Hug, Phys. Rev. B **74**, 174501 (2006).
[34]S. Amini, A. Zhou, S. Gupta, A. DeVillier, P. Finkel, and M. W. Barsoum, J. Mater. Res. **23**, 2157 (2008).
[35]T. H. Scabarozi, A. Ganguly, J. D. Hettinger, S. E. Lofland, S. Amini, P. Finkel, T. El-Raghy, and M. W. Barsoum, J. Appl. Phys. **104**, 073713 (2008).
[36]S. Amini, M. W. Barsoum, and T. El-Raghy, J. Am. Ceram. Soc. **90**, 3953 (2007).
[37]B. Rupp, Scr. Metall. **22**, 69 (1988).
[38]C. A. Swenson, J. Phys. Chem. Ref. Data **12**, 179 (1983).
[39]NIST Standard Reference Material No. 736.
[40]G. Kresse and J. Furthmuller, Phys. Rev. B **54**, 11169 (1996).
[41]MedeA, 2.2.1 ed. (Materials Design, Angel Fire, NM).
[42]G. Kresse and D. Jouber, Phys. Rev. B **59**, 1758 (1999).
[43]P. E. Blöchl, Phys. Rev. B **50**, 17953 (1994).
[44]J. P. Perdew, K. Burke, and M. Ernzerhof, Phys. Rev. Lett. **77**, 3865 (1996).
[45]Y. Le Page and P. Saxe, Phys. Rev. B **65**, 104104 (2002).
[46]M. W. Barsoum, C. J. Rawn, T. El-Raghy, A. T. Procopio, W. D. Porter, H. Wang, and C. R. Hubbard, J. Appl. Phys. **87**, 8407 (2000).
[47]S. R. Kulkarni, M. Merlini, N. Phatak, S. K. Saxena, G. Artioli, S. Amini, and M. W. Barsoum, J. Alloys Compd. (in press).
[48]S. R. Kulkarni, M. Marco, N. Phatak, S. K. Saxena, G. Artioli, S. Gupta, and M. W. Barsoum, J. Am. Ceram. Soc. **90**, 3013 (2007).
[49]N. V. Tzenov and M. W. Barsoum, J. Am. Ceram. Soc. **83**, 825 (2000).
[50]T. El-Raghy, S. Chakraborty, and M. W. Barsoum, J. Eur. Ceram. Soc. **20**, 2619 (2000).
[51]M. W. Barsoum, I. Salama, T. El-Raghy, J. Golczewski, W. D. Porter, H. Wang, H. J. Seifert, and F. Aldinger, Metall. Mater. Trans. A **33A**, 2775 (2000).
[52]M. W. Barsoum, J. Golczewski, H. J. Seifert, and F. Aldinger, J. Alloys Compd. **340**, 173 (2002).
[53]A. Krajewski, L. D'Alessio, and G. D. Maria, Cryst. Res. Technol. **33**, 341 (1998).
[54]S. R. Kulkarni, R. S. Vennila, N. A. Phatak, S. K. Saxena, C. S. Zha, T. El-Raghy, M. W. Barsoum, W. Luo, and R. Ahuja, J. Alloys Compd. **448**, L1 (2008).
[55]M. Radovic, A. Ganguly, and M. W. Barsoum, J. Mater. Res. **23**, 1517 (2008).
[56]C. R. Houska, J. Phys. Chem. Solids **25**, 359 (1964).
[57]N. A. Dubrovinskaia, L. S. Dubrovinsky, S. K. Saxena, R. Ahuja, and B. Johansson, J. Alloys Compd. **289**, 24 (1999).
[58]H. O. Pierson, *Handbook of Refractory Carbides and Nitrides* (Noyes, Westwood, NJ, 1996).
[59]H. P. Liermann, A. K. Singh, B. Manoun, S. K. Saxena, V. B. Prakapenka, and G. Shen, Int. J. Refract. Met. Hard Mater. **22**, 129 (2004).
[60]C. R. Hquska, J. Am. Ceram. Soc. **47**, 310 (1964).
[61]H. P. Liermann, A. K. Singh, M. Somayazulu, and S. K. Saxena, Int. J. Refract. Met. Hard Mater. **25**, 386 (2007).
[62]H. L. Brown, P. E. Armstrong, and C. P. Kempter, J. Chem. Phys. **45**, 547 (1966).
[63]A. I. Gusev, A. A. Rempel, and A. J. Magerl, *Disorder and Order in Strongly Nonstoichiometric Compounds: Transition Metal Carbides, Nitrides, and Oxides* (Springer, New York, 2001).
[64]T. H. K. Barron, J. G. Collins, and G. K. White, Adv. Phys. **29**, 609 (1980).
[65]J. Wang and Y. Zhou, Phys. Rev. B **69**, 214111 (2004).
[66]A. T. Procopio, M. W. Barsoum, and T. El-Raghy, Metall. Mater. Trans. A **31A**, 333 (2000).
[67]B. Manoun, F. X. Zhang, S. K. Saxena, M. W. Barsoum, and T. El-Raghy, J. Phys. Chem. Solids **67**, 2091 (2006).
[68]A. Onodera, H. Hirano, T. Yuasa, N. F. Gao, and Y. Miyamoto, Appl. Phys. Lett. **74**, 3782 (1999).
[69]J. E. Spanier, S. Gupta, M. Amer, and M. W. Barsoum, Phys. Rev. B **71**, 012103 (2005).
[70]D. L. Anderson and O. L. Anderson, J. Geophys. Res. **75**, 3494 (1970).
[71]A. Jayaraman, B. Batlogg, R. G. Maines, and H. Bach, Phys. Rev. B **26**, 3347 (1982).
[72]L. Lopez-de-la-Torre, B. Winkler, J. Schreuer, K. Knorr, and M. Avalos-Borja, Solid State Commun. **134**, 245 (2005).
[73]G. Hug, M. Jaoun, and M. W. Barsoum, Phys. Rev. B **71**, 024105 (2005).
[74]Z. M. Sun and Y. C. Zhou, Phys. Rev. B **60**, 1441 (1999).
[75]Z. Sun, S. Li, R. Ahuja, and J. M. Schneider Solid State Commun. **129**, 589 (2004).
[76]B. Holm, R. Ahuja, and B. Johansson, Appl. Phys. Lett. **79**, 1450 (2001).
[77]Y. C. Zhou, Z. M. Sun, X. H. Wang, and S. Q. Chen, J. Phys. Condens. Matter **13**, 10001 (2001).
[78]J. M. Schneider, Z. Sun, R. Mertens, F. Uestel, and R. Ahuja Solid State Commun. **130**, 445 (2004).
[79]J. Y. Wang and Y. C. Zhou, Phys. Rev. B **69**, 144108 (2004).
[80]J. Y. Wang and Y. C. Zhou, J. Phys. Condens. Matter **16**, 2819 (2004).
[81]Z. M. Sun, D. Music, R. Ahuja, and J. M. Schneider, J. Phys. Condens. Matter **17**, 7169 (2005).